This is an open access article published under a Creative Commons Non-Commercial No Derivative Works (CC-BY-NC-ND) Attribution License, which permits copying and redistribution of the article, and creation of adaptations, all for non-commercial purposes.

ACS AUTHORCHOICE

ACS OMEGA

http://pubs.acs.org/journal/acsodf

Article

Equilibria and Isosteric Heat of Adsorption of Methane on Activated Carbons Derived from South African Coal Discards

Jibril Abdulsalam,* Jean Mulopo, Samson Oluwaseyi Bada, and Bilainu Oboirien

Cite This: *ACS Omega* 2020, 5, 32530−32539

Read Online

ACCESS | Metrics & More | Article Recommendations

ABSTRACT: Isosteric heat of adsorption (H_{st}) is critical for evaluating the thermal effects of adsorption-based storage systems. Poor management of the thermal effects of an adsorptive storage system often alters the overall performance of the storage system. In this study, methane equilibrium uptake on activated carbons derived from coal discards and isosteric heat of adsorption were evaluated. The methane adsorption capacity of the produced activated carbons was measured using a high-pressure volumetric analyzer. The isotherm results in temperature ranges of 0−50 °C and pressure of up to 40 bar are analyzed using the Langmuir, Tóth, and Dubinin−Astakhov (DA) isotherm models. The results showed that, for the two activated carbons, the DA model was the best fit. In addition, we evaluated the isosteric heat of adsorption using two theoretical frameworks, Maxwell's thermodynamic relations and the modified Polanyi potential function. The Tóth potential function and Clausius−Clapeyron equations were applied to the Dubinin−Astakhov adsorption model to obtain an analytical expression of H_{st}. Both methods were compared, and the result showed an overall error margin between 6 and 12%. The values of H_{st} obtained are over a range of 10−17 kJ/mol. It was observed that H_{st} decreases with an increase in methane fractional load. The H_{st} values obtained are useful in designing an efficient thermodynamic scheme for the ANG storage system.

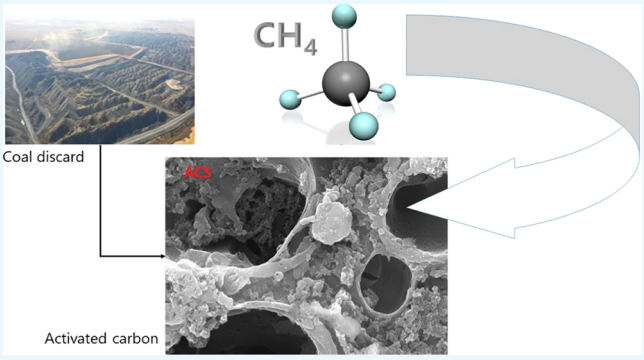

1. INTRODUCTION

Interest in natural gas as an alternative energy source has grown considerably over the years.

Natural gas can be substituted for petroleum or integrated with petroleum as a hybrid vehicle with low emission. Nations that want to reduce their dependence on imported crude oil are looking to natural gas to meet their rising energy demand. To meet this requirement, an appropriate storage system is needed to promote access to and improve the use of natural gas. The existing form of storing natural gas is as compressed natural gas (CNG) and as liquefied natural gas (LNG).[1] The gas is stored in a cylindrical vessel at 200−250 bar in the CNG system. However, in the LNG system, the gas is condensed to a liquid and then stored in storage tanks at a temperature of about −162 °C. The two approaches require high investment cost, high pressure, and high energy, and raise huge safety concerns.[2]

The application of an adsorbed natural gas (ANG) storage system is a viable alternative to the abovementioned existing storage systems. The ANG system involves the storage of natural gas on porous materials packed in a storage tank at lower pressure. The technology enables the storage of the same amount of gas as that stored in a CNG system at a much lower pressure.[3] The storing of gas at a lower pressure offers two major competitive advantages; lower energy for compression and design flexibility, leading to the ease of modifying storage tanks. Furthermore, since ANG uses porous materials for storing gas, this gives higher energy density and greater storage capacity.[4]

In sorptive storage applications, advanced porous materials such as activated carbon have gained considerable attention due to their extremely high surface areas and chemically tunable structures.[5] Considerable efforts have been made to produce activated carbons suitable for the ANG storage system.[6,7] Activated carbons are typically produced via the physical or chemical activation process, using raw materials such as coals, coconut shells, oil palm shells, rice husks, etc. In a study conducted by Arami-Niya et al.,[8] the authors reported the maximum methane adsorption of 12 cm^3/g at 1 bar using granular activated carbon produced via chemical activation of oil palm shell using $ZnCl_2$. Alcañiz-Monge et al.[5] investigated the adsorption of methane at 298 K and 4 MPa on microporous activated carbon (AC), activated carbon fibers (ACFs), and super activated carbon (SAC). The author reported a maximum

Received: September 28, 2020
Accepted: November 10, 2020
Published: December 9, 2020

ACS Publications

© 2020 The Authors. Published by American Chemical Society

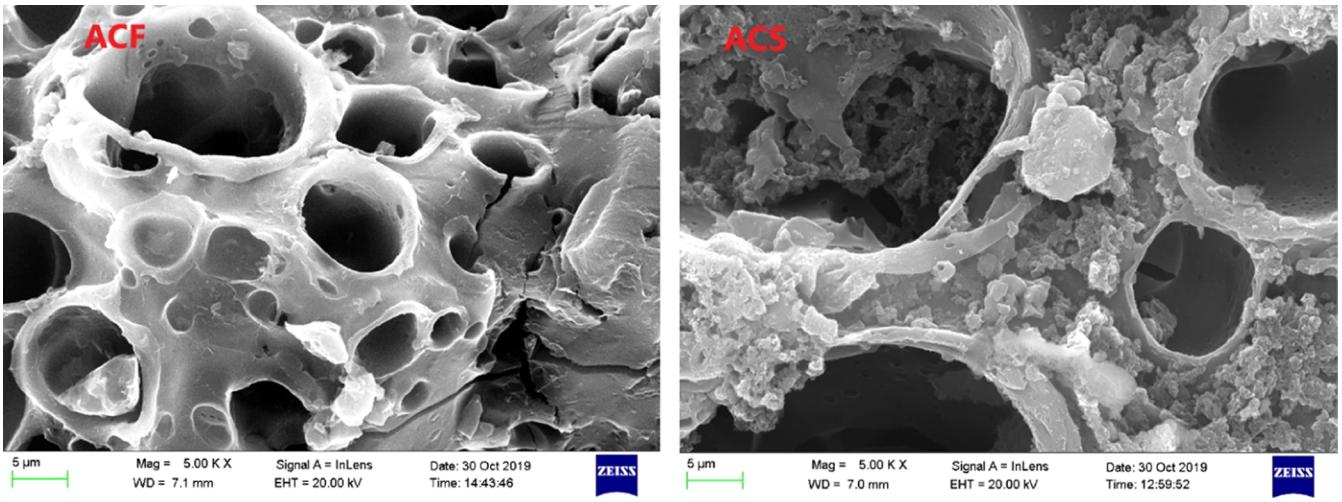

Figure 1. SEM images of the activated carbons (ACF and ACS).

storage capacity of 13 mmol/g (291.4 cm^3/g) with SAC due to its large surface area of 3790 m^2/g and a high micropore volume of 1.9 cm^3/g. Sreńscek-Nazzal et al.[9] reported methane storage capacity of 181.61 mg/g at 40 bar and 197.23 mg/g at 50 bar using activated carbon produced by chemical activation of sugarcane molasses with KOH. The findings of these studies suggest that activated carbons have high potential for storing methane.

The assessment of the adsorption process is usually based on two factors, the adsorption isotherm and heat of adsorption.[10−12] The adsorption capacity is measured from the isotherm, while the heat of adsorption shows how strongly the adsorbate is attracted to the solid adsorbent surface. In general, macro-thermodynamics or statistical mechanics can be used to evaluate the adsorption equilibrium of natural gas on adsorbents. While the former is described by adsorption models, the latter is primarily based on molecular simulations.[13] Because of the high accuracy of adsorption data prediction, the use of adsorption models in the study of the adsorption equilibrium is an important approach for adsorptive system design.[14]

The change in enthalpy obtained from the isotherm of adsorption at two or more temperatures is known as the isosteric heat of adsorption. It is also defined as heat distributed to the surrounding environment when a discreet volume of gas is transferred from its bulk gas phase to its adsorbed phase under the conditions of constant temperature and pressure.[15] Builes et al.[16] described isosteric heat as the difference between species i partial molar enthalpies in the bulk fluid phase and the adsorbed phase.

$$\Delta H_i^{st} = \bar{H}_i^b - \bar{H}_i^a \quad (1)$$

Where b is the bulk fluid phase and a is the adsorbed phase.

Studies have been carried out on the prediction of the adsorption isosteric heat. Some of these studies used the conventional Clausius−Clapeyron equation for estimating the isosteric heat of adsorption. This equation is often applied to the isotherm model that best fits the isotherm data.[17,18] Zhu and Zheng[13] measured the isosteric heat of methane adsorption on three separate adsorbents (graphene sheets, activated carbon, and carbon black) using the Clausius−Clapeyron equation. The study showed that the isosteric heat of methane adsorption on the activated carbon was 21.62, 21.78, and 21.94 kJ/mol at 253.15, 273.15, and 293.15 K, respectively. The study also showed that an adsorbent with a larger specific surface area has a higher amount of adsorption and greater isosteric heat of adsorption. Another investigation conducted by Balathanigaimani et al.[19] used the Clausius−Clapeyron equation to measure the isosteric heat of methane adsorption on activated carbon produced from rice husk. The study results showed that the isosteric heat of methane adsorption on activated carbon ranged from 20.6 to 46 kJ/mol at different surface loadings. Ning et al.[20] reported isosteric heat of 5−22.5 kJ/mol for methane adsorption on activated carbon produced by chemical activation of coconut shell with K_2CO_3. However, the use of the Clausius−Clapeyron equation requires isotherm data at different temperatures, which makes it complex and time-consuming.[21]

Molecular simulation has been applied in predicting isosteric heat in numerous investigations. Herdes et al.[22] used a Monte Carlo simulation to estimate the isosteric heat of 2,2-dimethylpropane (C_5H_{12}) adsorption at low pressure. An adequate approximation that is suitable for isosteric heat prediction, especially when it is difficult to quantify experimentally, was reported by the author. Another study by Birkett and Do[23] estimated the isosteric heat of water adsorption on carbon black. The study showed that molecular simulation offers a satisfactory approach for predicting the isosteric heat of adsorption. However, the use of molecular simulation is complex and requires experimental results to verify the model.[21]

A more recent approach is the equation derived from Tóth's potential theory.[21] The distinction between this equation and the Clausius−Clapeyron equation is that the Clausius−Clapeyron relationship is based on Maxwell's thermodynamic relationship, whereas Tóth's potential function is an empirical relationship that uses a modified form of the Polanyi potential function. This method requires the measurement of only a single isotherm, in contrast to the Clausius−Clapeyron method, which requires multiple isotherms.[24] Whittaker et al.[21] developed this equation and applied it to the Langmuir and Tóth isotherm models to estimate the isosteric heat of adsorption on solid adsorbents using a single isotherm data. The findings from the study revealed that the method offers a satisfactory prediction of isosteric heat with an error margin of 10−15%. The findings of these studies demonstrate the adequacy of the Clausius−Clapeyron equation and the Tóth potential function in estimating the isosteric heat of gas adsorption on solid adsorbents such as activated carbons. The general conclusion

https://dx.doi.org/10.1021/acsomega.0c04744
ACS Omega 2020, 5, 32530−32539

is that the results of these methods provide reasonable estimates of isosteric heat of adsorption.

In our previous studies,[4,25] we have shown that South African coal discards are good raw materials for the preparation of activated carbons by chemical activation, which enables high adsorption capacity to be achieved with porosity (mostly including micropores). These activated carbons can be interesting for methane storage applications. Thus, based on our previous results, the objective of the present work is to characterize activated carbons produced from South African coal discards through a key basic thermodynamic property, namely the isosteric heat of adsorption. Accurate knowledge of the isosteric heat of adsorption is crucial for the simulation of thermal effects in adsorption-based storage systems using conventional software packages such as Aspen Plus, gPROMS, etc. Managing the thermal effects is a very significant aspect for improving the efficiency and efficacy of adsorption storage systems as their misrepresentation can affect the prediction of the overall efficiency of the heating system. On the other hand, the knowledge of isosteric heat of adsorption allows the understanding of the ability of the synthesized material to dissipate the heat produced in the system more or less rapidly, thus, helping better estimation of the methane recharge period. For the above reasons, this paper models the isosteric heat of adsorption of the synthesized activated carbons using the Clausius−Clapeyron relationship and Tóth's potential theory. This approach has the clear advantage of deriving analytical expressions for the isosteric heat of adsorption, which can be integrated into the calculation algorithms of adsorption equipment as implemented in modern process simulators, i.e. Aspen Plus and gPROMS. This approach also provides a preliminary platform to assess the ability of adsorption models to explain both the adsorption isotherms and the isosteric heat at the same time. The contribution of such an approach is that it helps in better understanding the adsorption process in relation to its energy component.

2. RESULTS AND DISCUSSION

2.1. Analysis of Surface Characteristics. Figure 1 shows the SEM image of the activated carbons used in this study. The activated carbons are labeled ACF (activated carbon from coal fines) and ACS (activated carbon from coal slurry). Well-developed pores are seen clearly on the surface of the activated carbons, as shown in Figure 1. Pores are important because they increase the surface area and pore volume of activated carbon and thus increase the methane adsorption capacity. This is in agreement with the findings reported by Omri and Benzina,[26] Lillo-Ródenas et al.,[27] and Linares-Solano et al.[28] SEM analysis confirms that the activated carbons are highly porous with pores of various sizes.

Figure 2 shows the nitrogen (N_2) adsorption−desorption isotherms of the activated carbons used in this study. The isotherms were observed to be type IV isotherm.[29] The isotherms are characterized by volumes adsorbed at lower P/P_o, followed by a knee, an indication of micropores with a wide pore diameter, and a horizontal plateau. The knee is a result of steady pore filling, which is similar to the isotherm obtained by Zhao et al.[30] The adsorption of N_2 at low relative pressure and higher relative pressure with a horizontal plateau suggests an adsorbent containing micropores and mesopores.[31] The adsorption at low relative pressure is attributed to increased adsorbent−adsorbate interactions in narrow micropores resulting in micropore filling at low relative pressure.[32]

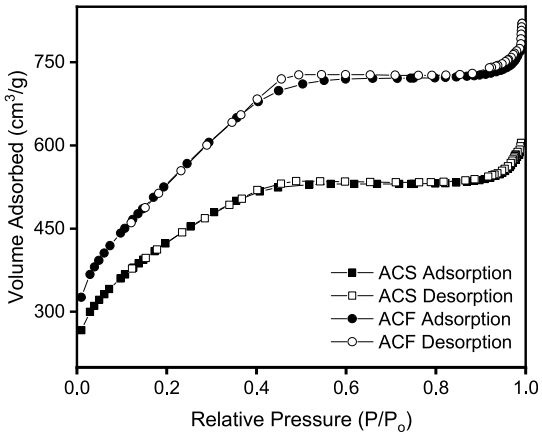

Figure 2. N_2 adsorption−desorption plot of the activated carbons (ACF and ACS).

The physical properties of the activated carbons (ACF and ACS) are listed in Table 1. The nitrogen adsorption capacity of activated carbons varies considerably. This provides a correlation between the surface area and the volume of nitrogen adsorbed. The larger the surface area, the higher the adsorption capacity of the activated carbon. This is consistent with the findings reported by Panella et al.[33] and Bénard and Chahine.[34] The studies showed that the nitrogen adsorption capacity correlates to the surface area for many carbon materials. Düren et al.[35] used computational methods to measure the adsorption capacity and surface area of various carbon materials and found that the surface area is an important property that influences gas adsorption.

Table 1. Physical and Structural Properties of Activated Carbons

properties	ACF	ACS
surface area (m^2/g)	1826.41	1484.96
pore volume (cm^3/g)	1.252	1.042
pore diameter (nm)	2.66	2.51
density (kg/m^3)	2241.9	2491.4

2.2. Adsorption Experiments. Adsorption studies were conducted at different pressures between 0 and 40 bar and at three temperatures, i.e., 0, 25, and 50 °C. The results showed that the methane uptake increased with an increase in pressure and a decrease in temperature. The amount of methane adsorbed on the two activated carbons is presented in Tables 2 and 3. The maximum adsorbed volume of methane was obtained at an average pressure of 37 bar at each temperature for both activated carbons. The amount of methane adsorbed by ACF is greater than that by ACS. This may be due to the larger surface area and a larger pore volume of ACF. This observation is consistent with the results obtained by Düren et al.,[35] Loh et al.,[36] Martin et al.,[37] and Rahman et al.[38]

2.3. Adsorption Isotherm Models. Methane adsorption data for the two activated carbons were regressed using nonlinear regression with the Langmuir, Tóth, and DA models. A programming code written in MATLAB by Do[39] was modified and used for fitting the experimental data to the models. To demonstrate the suitability of the model equations, the experimental data was plotted against the model data. The error of regression between the experimental data and the model data was obtained using the following equation[36]

https://dx.doi.org/10.1021/acsomega.0c04744
ACS Omega 2020, 5, 32530−32539

Table 2. Experimental Data for Methane Adsorption on ACF[a]

T = 0 °C		T = 25 °C		T = 50 °C	
pressure (bar)	ads. vol. (mol/kg)	pressure (bar)	ads. vol. (mol/kg)	pressure (bar)	ads. vol. (mol/kg)
0.8	1.00	0.8	0.51	0.8	0.38
3.3	3.03	3.3	1.71	3.3	1.30
7.4	4.99	7.4	3.02	7.4	2.33
12.0	6.34	12.0	4.08	12.1	3.21
17.0	7.21	16.9	4.90	17.0	3.90
21.8	7.75	21.8	5.60	21.8	4.49
26.8	8.00	26.9	6.15	26.9	5.03
31.8	8.04	32.0	6.63	31.8	5.49
36.8	8.08	37.0	7.03	36.9	5.98

[a]Ads. vol.: Adsorbed Volume.

Table 3. Experimental Data for Methane Adsorption on ACS

T = 0 °C		T = 25 °C		T = 50 °C	
pressure (bar)	ads. vol. (mol/kg)	pressure (bar)	ads. vol. (mol/kg)	pressure (bar)	ads. vol. (mol/kg)
0.8	0.66	0.8	0.43	0.8	0.23
3.4	2.00	3.4	1.35	3.4	1.27
7.5	3.26	7.5	2.27	7.5	2.15
12.1	4.14	12.1	2.98	12.2	2.63
17.1	4.74	17.0	3.53	17.0	3.01
22.0	5.13	21.9	3.95	22.0	3.18
26.9	5.36	26.9	4.28	26.9	3.28
31.9	5.42	31.8	4.56	31.9	3.35
37.1	5.55	36.8	4.76	36.8	3.38

$$\text{error of regression} = \frac{\sqrt{\frac{1}{N}\sum_{i=1}^{N}(C_{\text{experiment}} - C_{\text{model}})^2}}{\frac{1}{N}\sum_{i=1}^{N} C_{\text{experiment}}} \quad (2)$$

where N is the number of data points.

The model predicted values and experimental data for all models are shown in Figures 3 and 4. An increase in temperature is observed to reduce the volume of methane adsorbed on the two activated carbons. This has to do with the fact that the adsorbed molecule gains higher energy at higher temperatures, causing it to evaporate.[39,40] The Figures reveal that all isotherms have the characteristic of type I isotherm of adsorption. It is also observed that the three models (Langmuir, Tóth, and DA) are

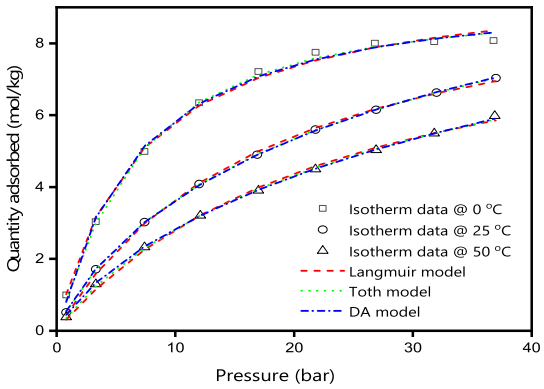

Figure 3. Fitting of methane/ACF adsorption data to Langmuir, Tóth, and DA models.

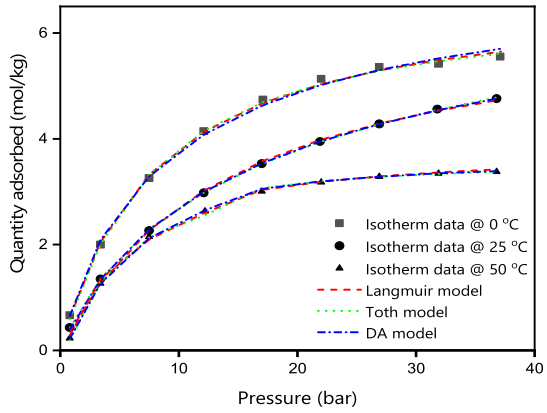

Figure 4. Fitting of methane/ACS adsorption data to Langmuir, Tóth, and DA models.

sufficiently reliable to estimate the adsorbed volume of methane on the activated carbons with a regression error of less than 3% (Tables 4 and 5).

Table 4. Langmuir, Tóth, and DA Isotherm Constants for the Adsorption of Methane on ACF[a]

isotherm parameters	0 °C	25 °C	50 °C
	Langmuir		
$C_{\mu s}$ (mol/kg)	9.966	10.394	9.748
b (bar^{-1})	0.1415	0.0545	0.0407
EoR (%)	2	1.43	2.23
R^2	0.9958	0.9993	0.9983
	Tóth		
$C_{\mu s}$ (mol/kg)	9.171	14.784	13.41
b (bar^{-1})	0.1206	0.0521	0.0372
t	1.31	0.67	0.71
EoR (%)	2.43	1.58	0.83
R^2	0.9979	0.9984	0.9963
	DA		
W_o (mol/kg)	8.8708	9.7258	9.0664
E (kJ/mol)	4.2495	3.0457	2.7141
n	2.6	1.6	1.4
EoR (%)	1.15	0.12	0.64
R^2	0.9996	0.9999	0.9998

[a]$C_{\mu s}$ − maximum adsorbed volume; b − the affinity constant; EoR − Error of Regression; t − Tóth equation parameter; W_o − saturated adsorbed volume; E − characteristic energy of adsorption; n − heterogeneity parameter; and R^2 − coefficient of determination.

Tables 4 and 5 show the numerical values of the adsorption parameters and percentage error of the regression, and the goodness of fit (R^2) of Langmuir, Tóth, and DA models for ACF and ACS.

Tables 4 and 5 shows that the affinity constant (b) of the Langmuir and Tóth models, which is an indicator of how much the methane molecule is drawn to the activated carbon surface, decreases with an increase in temperature for the two activated carbons. Do[39] stated that the higher the value of b, the more the adsorbent surface is covered by adsorbate molecules due to the higher attraction of the adsorbate molecules to the adsorbent surface. The results presented in Tables 4 and 5 are consistent with this statement. The highest value of b and the highest adsorbed volume of methane was obtained at 0 °C for the two activated carbons. Parameter "t" of the Tóth model describes the heterogeneous nature of the adsorbate−adsorbent system

https://dx.doi.org/10.1021/acsomega.0c04744
ACS Omega 2020, 5, 32530−32539

Table 5. Langmuir, Tóth, and DA Isotherm Constants for the Adsorption of Methane on ACS

isotherm parameters	0 °C	25 °C	50 °C
	Langmuir		
$C_{\mu s}$ (mol/kg)	6.863	6.538	3.843
b (bar^{-1})	0.1251	0.0709	0.0308
EoR (%)	1.64	1.48	2.23
$R2$	0.9983	0.9993	0.9962
	Tóth		
$C_{\mu s}$ (mol/kg)	6.558	8.662	3.578
b (bar^{-1})	0.1186	0.0744	0.0617
t	1.12	0.68	1.32
EoR (%)	1.45	1.38	1.46
$R2$	0.9988	0.9982	0.9936
	DA		
W_o (mol/kg)	6.4119	5.9092	3.5108
E (kJ/mol)	4.0483	3.4475	4.7074
n	2.1	1.8	2.9
EoR (%)	1.17	0.36	0.93
$R2$	0.9997	0.9998	0.9970

(methane-activated carbon in this study). The more the value of t deviates below 1, the higher the degree of heterogeneity of the system.[39] Based on the value of t shown in Tables 5 and 6, the methane−ACF and methane−ACS systems are found to be more heterogeneous at 25 °C.

The parameter "n" of the DA model is an indication of the surface heterogeneity of the adsorbents, with the values of n varying between 1.4 and 2.9 for the two activated carbons at different temperatures. Do[39] reported that the value of n less than 3 describes a heterogeneous solid with a wide micropore size distribution. This suggests that the two activated carbons (ACF and ACS) in this study are heterogeneous with a wide micropore size distribution at different temperatures.

Table 6. Isosteric Heat of Methane Adsorption on Various Adsorbents

adsorbents	isosteric heat of adsorption (kJ/mol)	temperature (°C)	reference
silicalite-I	18−28	30−80	45
NaETS-4	29.3	15−45	46
heulandite	19	25	47
chabazite	15	25	47
DD3R zeolite	19	0−75	48
MWCNT	18−40	30−50	49
MWCNT	11.47−41.47	10−45	41
MWCNT	5.8−9.1	10−45	41
activated carbon	8.45−27.5	27−45	37
activated carbon	21.62−21.94	−20−20	13
activated carbon	11−24	25−50	20
activated carbon	5−22.5	25−50	20
activated carbon	15.78−16.72	0−100	50
activated carbon	15.94−18.26	0−100	50
activated carbon	15.83−16.97	0−100	50
activated carbon	25	20−50	51
activated carbon	14.7−17.4	0−100	52
ACF, ACS	10−17	0−50	this study

2.4. Isosteric Heat of Adsorption Study. The two activated carbons under study are heterogeneous, as shown by the parameters of the Tóth and DA models. However, the DA model provides the best fit for the isotherm data with the lowest regression error and the highest R^2 value, so the DA equation is considered more suitable for estimating the isosteric heat of adsorption. The DA model parameters (Tables 4 and 5) were then used for the estimation of isosteric heat at the various temperatures using the Clausius−Clapeyron equation (eqs 12 and 13) and the Tóth potential function equation (eqs 18 and 19). The results are presented as a plot of isosteric heat of adsorption versus fractional loading, as shown in Figures 5 and 6.

The isosteric heat of adsorption obtained at different temperatures is in the range of 10−17 kJ/mol for the two activated carbons. As a rule of thumb, the heat of adsorption of 80 kJ/mol or more indicates chemisorption, and lower values indicate physisorption.[41,42] The values of isosteric heat of adsorption obtained in this study are below 80 kJ/mol indicating that methane adsorption on the activated carbons is physisorption.

Figures 5 and 6 show the plots of isosteric heat as a function of fractional loading of methane on the two activated carbons (ACF and ACS). The symbols represent the isosteric heat calculated using the Clausius−Clapeyron equation, while the solid lines represent isosteric heat calculated using the Tóth potential function equations. As can be seen in these figures, the isosteric heat of adsorption varies with surface loading. Based on isosteric heat at low surface loading, ACF is marginally higher than ACS, which is more pronounced at 50 °C.

As shown in Figures 5 and 6, the calculated isosteric heat from the Clausius−Clapeyron and the Tóth potential function equations followed the same trend, showing that the isosteric heat decreases with an increase in methane loading. Methane molecules first penetrate smaller pores at the initial stage of adsorption, resulting in a stronger interaction between methane and active sites on the adsorbent surface. This results in high isosteric heat at lower loading. With an increase in loading, the interaction between methane and the adsorbent surface decreases due to pore filling, which leads to a decrease in the isosteric heat of adsorption. This is in agreement with the report of Do,[39] which notes that an indication of solid heterogeneity is a decrease in the isosteric heat of adsorption with an increase in adsorbate loading due to the adsorbate filling the higher energy sites first, then the lower energy sites are steadily filled up as the gas pressure increases.[39]

As can be seen in Figures 5 and 6, the values calculated using the Clausius−Clapeyron equation and the Tóth potential function equations were observed to be in agreement with each other with an average error range of 6−12% at different temperatures. The margin of error between the calculated values using the two equations is 10, 8, and 12% for ACF at 0, 25, and 50 °C, while it is 6.6, 7, and 9.6% for ACS at 0, 25, and 50 °C respectively. However, studies by Whittaker[24] and Aremu[44] reported that the values of isosteric heat obtained using the Tóth potential function equation were closer to the measured calorimetric values with an error margin of 10−15%.

The isosteric heat of adsorption of the two activated carbons is comparable to the isosteric heat of adsorption obtained in a previous study by Loh et al.[36] in the range of 11.97−13.39 kJ/mol for methane adsorption on two commercial activated

https://dx.doi.org/10.1021/acsomega.0c04744
ACS Omega 2020, 5, 32530−32539

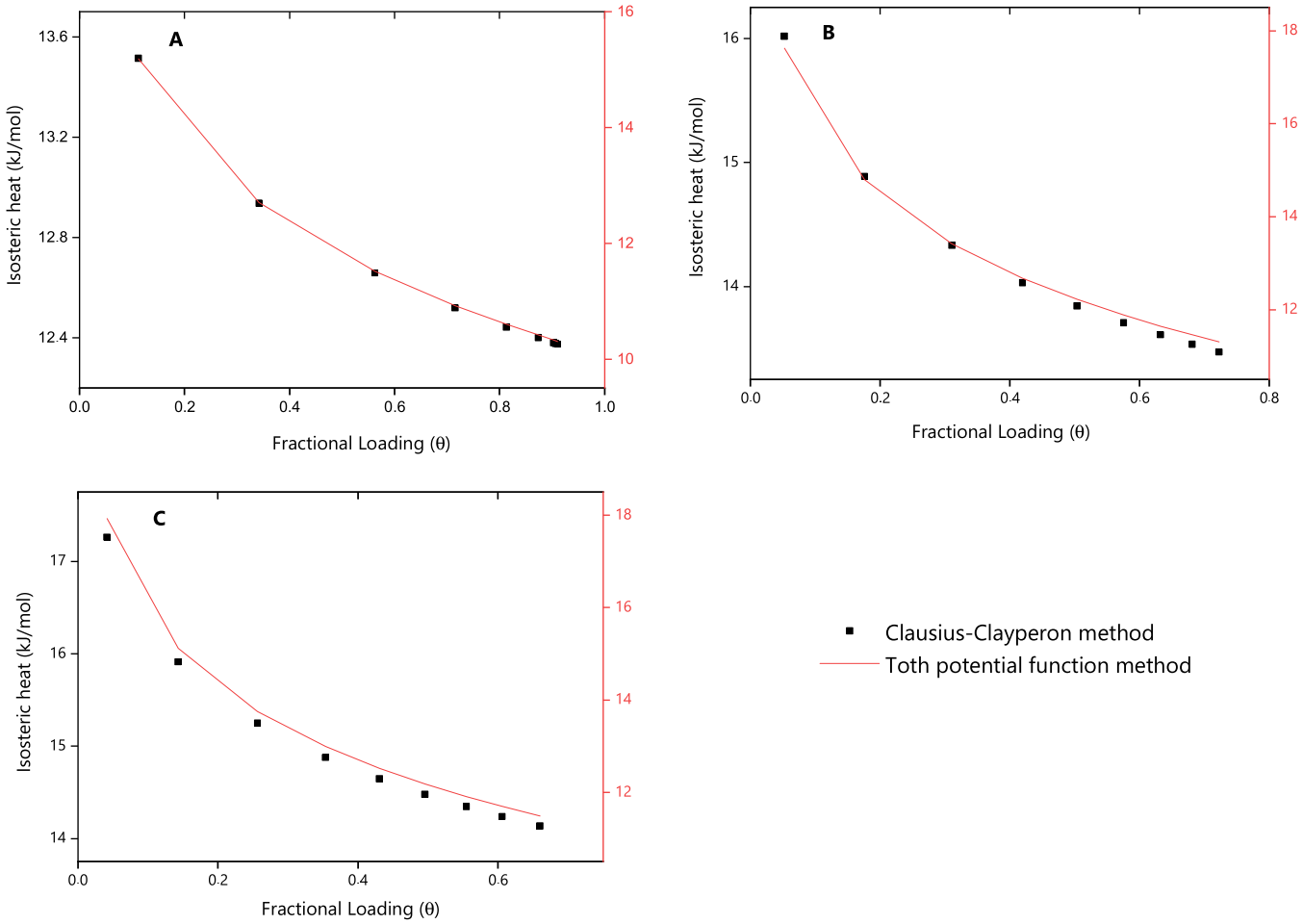

Figure 5. Isosteric heat data of methane on ACF at (A) 0 °C, (B) 25 °C, and (C) 50 °C.

carbons, Maxsorb III and ACF-A20. The result of this is that, relative to Maxsorb III and ACF-A20, the use of ACF and ACS as adsorbents in the ANG storage system will slightly increase the thermal load of the system. Adsorbents with low heat of adsorption are preferred in the ANG storage system.[19] It is also worth noting that the values of the isosteric heat obtained in this study are comparable to other values reported in the literature, as shown in Table 6.

3. CONCLUSIONS

Methane adsorption isotherms of activated carbons synthesized from South African coal discards were measured at pressures of up to 40 bar and temperatures of 0, 25, and 50 °C using a high-pressure volumetric apparatus. The main findings of the study can be summarized as follows:

- The experimental results of methane adsorption were validated with three isotherm models, Langmuir, Tóth, and DA. The DA model was found to be better suited to the isotherm data, with the lowest regression error of 0.64 and 0.82% for ACF and ACS, respectively.
- Clausius−Clapeyron equation and Tóth potential function were used to calculate the isosteric heat of adsorption. The estimated isosteric heat of adsorption ranged from 10 to 17 kJ/mol, which is comparable to the values reported in the literature. The calculated values obtained using the Clausius−Clapeyron and Tóth potential function equations were close. The Tóth potential function has the advantage of simplicity and ease of use since it requires only one isotherm data.
- The adsorption characteristics (adsorption isotherms and isosteric heat of adsorption) of methane on activated carbons are important for designing an effective ANG storage system. Developing activated carbons from South African coal discards to meet ANG adsorbent requirement will require an emphasis on enhancing its surface area and pore volume.

4. MATERIALS AND METHODS

4.1. Methane. The methane gas used was supplied by African Oxygen Ltd (AFROX), Johannesburg, South Africa. The accompanying certificate of analysis indicated a purity level of 99.95−100% of methane with other components as N_2 < 200 ppm, O_2 < 30 ppm, other hydrocarbons (OHC) < 300 ppm, and H_2 < 20 ppm.

4.2. Characterization of Activated Carbons. Activated carbons used in this study were produced from South African coal discards (waste from the coal beneficiation process in fines and slurry forms), which were synthesized using the chemical activation process. The collection and preparation of the samples were described in our previous works.[4,25] The composition of the raw coal discards used is listed in Table 7.

Scanning electron microscopy (SEM) analysis was carried out on activated carbons to study the surface morphology and pore development. The physical properties were measured by the

https://dx.doi.org/10.1021/acsomega.0c04744
ACS Omega 2020, 5, 32530−32539

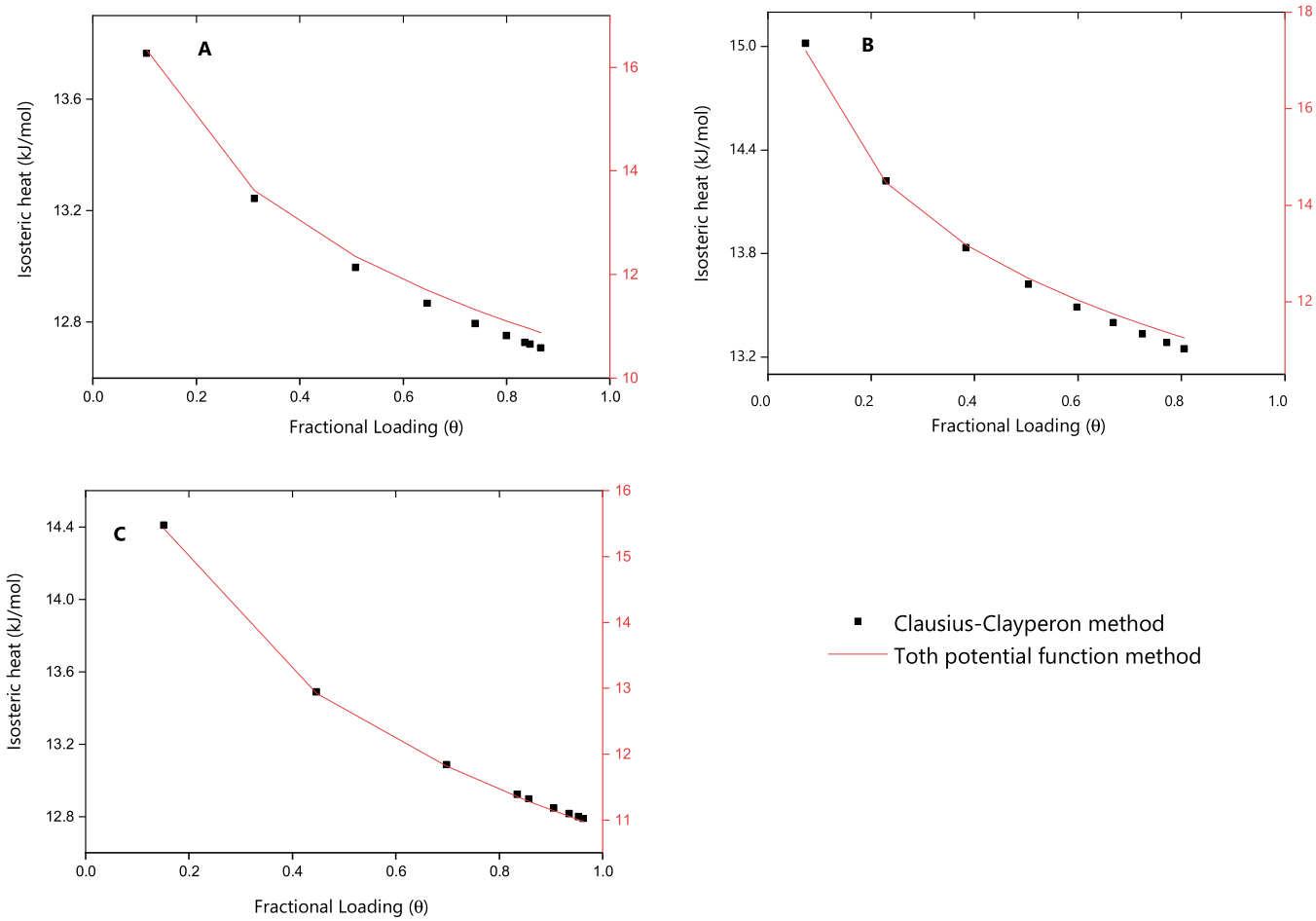

Figure 6. Isosteric heat data of methane on ACS at (A) 0 °C, (B) 25 °C, and (C) 50 °C.

Table 7. Proximate and Ultimate Analysis of Coal Discards[a]

analysis	coal fines (CF)	coal slurry (CS)
Proximate Analysis (wt %, adb)		
moisture content	2.1	2.6
ash	35.4	36.3
volatile matter	20	20.8
fixed carbon	42.5	40.3
Ultimate Analysis (wt %, adb)		
carbon	48.90	48.90
hydrogen	2.67	2.84
nitrogen	1.15	1.21
oxygen	45.94	45.84
total sulfur (wt %, adb)	1.34	1.21

[a]adb − air-dried basis.

Brunauer−Emmett−Teller (BET) method using N_2 adsorption isotherms at 77 K. N_2 adsorption and desorption isotherms were measured in a relative pressure (P/P_o) range of 0.0001−0.99. This was used to measure the surface area, average pore diameter, and pore volume. The details of the characterization methods and equipment used are presented in our previous work.[25]

4.3. Adsorption Measurements. Measurement of methane adsorption on activated carbons at different temperatures of 0, 25, and 50 °C and pressures of up to 40 bars were carried out using a High-Pressure Volumetric Analyzer (HPVA II) from Particulate Systems. Figure 7 shows the schematic diagram of the HPVA equipment. A specified amount of gas is added into the sample chamber of the HPVA for analysis. When the equilibrium between the sample and the gas is reached, the equilibrium pressure is noted. The calculation of the amount of gas adsorbed by the sample is made using the equilibrium pressure data. Adsorption analysis is conducted repeatedly at specified pressure intervals until the specified maximum pressure is reached. To obtain adsorption isotherms, data on the amount of gas adsorbed is plotted against the equilibrium pressure.

4.4. Adsorption Isotherm Models. Three isotherm models, namely Langmuir, Tóth, and Dubinin−Astakhov were used to validate the methane adsorption experimental data. The Langmuir model is a simple model that describes the monolayer adsorption of the gas−solid phase, such as methane on activated carbon. The assumptions of the Langmuir isotherm model are: a homogeneous surface of the adsorbent; adsorption occurs within some localized sites, and the sites are all identical in each site and can contain one molecule at a time. The Langmuir theory is based on a kinetic principle, which states that the adsorption is equal to the rate of surface desorption.[39] The Langmuir model is written as

$$C_\mu = C_{\mu s}\frac{b(T)P}{1 + b(T)P} \tag{3}$$

where C_μ is the amount of adsorbed; $C_{\mu s}$ is a saturated amount of adsorbate adsorbed, subscript μ indicates the adsorbed phase and b is the affinity constant and is denoted as

https://dx.doi.org/10.1021/acsomega.0c04744
ACS Omega 2020, 5, 32530−32539

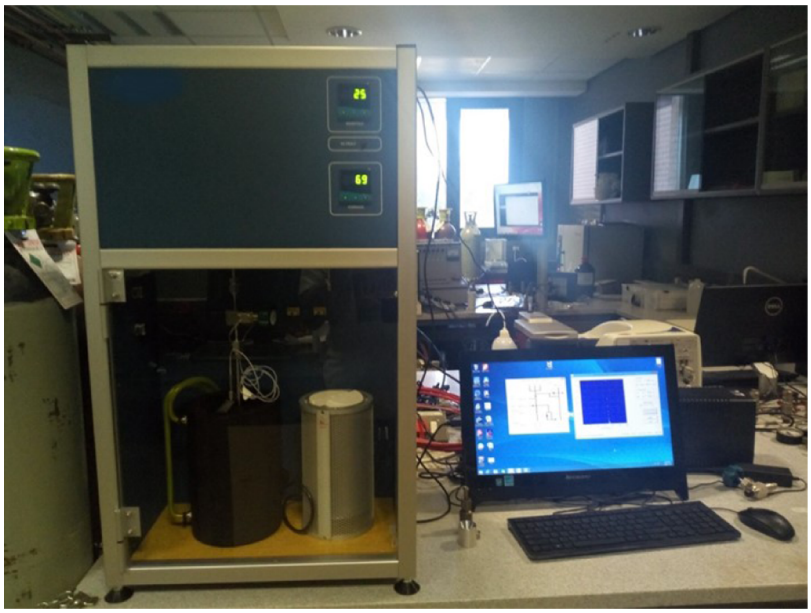

Figure 7. Image of the HPVA equipment.

$$b(T) = b_\infty \exp\left(\frac{Q}{R_g T}\right) \tag{4}$$

The Langmuir model is limited because it cannot precisely fit high-pressure adsorption data and does not describe the heterogeneity of the material.

The Tóth isotherm model was developed to improve and to resolve the constraints of the Langmuir model.[53] The Tóth model accurately fits low and high-pressure adsorption data and also describes the heterogeneity of the adsorbent. The Tóth equation is denoted as

$$C_\mu = C_{\mu s}\frac{bP}{[1 + (bP)^t]^{1/t}} \tag{5}$$

The exponent t is expressed as

$$t = t_0 + \alpha\left(1 - \frac{T_0}{T}\right) \tag{6}$$

where t is the parameter that describes the adsorbate−adsorbent system's heterogeneity,[39] t_o is the parameter t at some reference temperature T_o, and α is a constant parameter.

The Dubinin−Astakhov (DA) model is commonly used for describing the physisorption of several gases on activated carbons.[54,55] The DA model provides an adequate description of adsorption data of adsorbents with a high degree of heterogeneity and wider pore size distribution.[56] The DA equation is denoted as

$$W = W_0 \exp\left[-\left(\frac{A}{E}\right)^n\right] \tag{7}$$

where W is the amount of gas adsorbed, W_o is the saturated amount adsorbed, E is the characteristic energy of adsorption, and n is the Dubinin−Astakhov parameter that describes the surface heterogeneity of the adsorbent, and A is the adsorption potential and is denoted as

$$A = RT \ln\left(\frac{P_0}{P}\right) \tag{8}$$

Combining eqs 6 and 5, the DA equation becomes

$$W = W_0\left[-\left\{\frac{RT}{E}\ln\left(\frac{P_0}{P}\right)\right\}^n\right] \tag{9}$$

P_0 is the saturation pressure and is expressed as

$$P_0 = P_c\left(\frac{T}{T_c}\right)^2 \tag{10}$$

where P_c and T_c are the critical properties of the gas (methane in this study) at temperature T.

4.5. Calculation of Isosteric Heat. Isosteric heat is a measure of the strength of the interaction between the adsorbate molecules and the adsorbent surface.[13] The understanding of the isosteric heat of adsorption is an important and valuable criterion in the thermal management of an adsorption system.[37,57] One of the assumptions of the Langmuir isothermal model is that the energy of interaction between the adsorbate and the surface of the adsorbent is constant.[39] This is not valid for adsorbents that are heterogeneous in nature, as is the case with the materials used in this study.

The isosteric heat of adsorption can be calculated using the Clausius−Clapeyron equation. The Clausius−Clapeyron equation is represented as[39]

$$q_{st} = RT^2\left[\left(\frac{\partial(\ln P)}{\partial T}\right)_c\right] \tag{11}$$

where q_{st} is the isosteric heat. All other parameters are as previously described.

When the Clausius−Clapeyron equation is applied to the Tóth and DA models, the resulting equations are as follows[39,40]

Tóth model

$$q_{st} = q + \frac{\alpha}{n}RT^2[(1 + (bP)^n)\ln\theta - \ln(bP)] \tag{12}$$

DA model

https://dx.doi.org/10.1021/acsomega.0c04744
ACS Omega 2020, 5, 32530−32539

$$q_{st} = E\left[\ln\left(\frac{n_m}{n_a}\right)\right]^{1/m} + \lambda \tag{13}$$

The Tóth potential function method for isosteric heat calculation was based on the Polanyi potential function. The function relates the differential heat on an adsorbent that is homogeneous in nature using the equation

$$q_d \approx \varepsilon + \lambda \tag{14}$$

Where q_d is the differential heat of adsorption per mole of adsorbate, ε is the adsorption potential, and λ is the latent heat of vaporization.

The correction factor by Tóth[58] to eq 13 to account for the heterogeneous nature of an adsorbent is described by the equation:

$$\psi = \frac{n^s}{p}\frac{dp}{dn^s}\bigg|_T - 1 \tag{15}$$

Where n^s is adsorbate amount adsorbed per unit of adsorbent

Tóth corrected adsorption potential for monolayer coverage is given as

$$\Delta\lambda + RT\ln\left(\frac{\psi P^{sat}}{P}\right) \tag{16}$$

Whittaker et al.,[21] expressed the general form for the isosteric heat equation as

$$q_{st} \approx \Delta\lambda + \lambda_p + RT \tag{17}$$

Equations 17 and 18 show the isosteric heat equation when eq 16 is applied to the Tóth and DA isotherm models.[43,44] The details of the derivations are reported elsewhere.[43p,48−50]

$$q_{st} \approx RT\ln\left[\left(\frac{p^{sat}}{b^{1/m}}\right)\left(\frac{\theta^m}{(1-\theta^m)}\right)^{m-1/m}\right] + \lambda_p + RT \tag{18}$$

$$q_{st} \approx E\ln\left(\frac{n^*}{n^s}\right)^{1/m} + RT\ln\left[\frac{E\ln\left(\frac{n^*}{n^s}\right)^{1/m-1}}{mRT} - 1\right] + \lambda_p + ZRT \tag{19}$$

AUTHOR INFORMATION

Corresponding Author

Jibril Abdulsalam − *School of Chemical and Metallurgical Engineering, Faculty of Engineering and the Built Environment, University of the Witwatersrand, WITS, 2050 Johannesburg, South Africa;* orcid.org/0000-0001-5072-4996; Phone: +27 (0) 11 717 7571; Email: jibril.abdulsalam@wits.ac.za

Authors

Jean Mulopo − *School of Chemical and Metallurgical Engineering, Faculty of Engineering and the Built Environment, University of the Witwatersrand, WITS, 2050 Johannesburg, South Africa*

Samson Oluwaseyi Bada − *School of Chemical and Metallurgical Engineering, Faculty of Engineering and the Built Environment, University of the Witwatersrand, WITS, 2050 Johannesburg, South Africa*

Bilainu Oboirien − *Department of Chemical Engineering, University of Johannesburg, Johannesburg 2028, South Africa*

Complete contact information is available at: https://pubs.acs.org/10.1021/acsomega.0c04744

Notes

The authors declare no competing financial interest.

ACKNOWLEDGMENTS

The study is funded by the National Research Foundation (NRF) of South Africa. The SARChI Clean Coal Technology Grant (Grant no. 86421). The views, observations, and conclusions shared are those of the authors and must not be credited to the NRF.

REFERENCES

(1) Choi, W.-J.; Seo, J.-B.; Jang, S.-Y.; Jung, J.-H.; Oh, K.-J. Removal characteristics of CO2 using aqueous MEA/AMP solutions in the absorption and regeneration process. *J. Environ. Sci.* **2009**, *21*, 907−13.

(2) Alhasan, S.; Carriveau, R.; Ting, D.-K. A review of adsorbed natural gas storage technologies. *Int. J. Environ. Stud.* **2016**, *73*, 343−56.

(3) Pupier, O.; Goetz, V.; Fiscal, R. Effect of cycling operations on an adsorbed natural gas storage. *Chem. Eng. Process.* **2005**, *44*, 71−9.

(4) Abdulsalam, J.; Mulopo, J.; Bada, S.; Oboirien, B. Natural gas storage properties of adsorbents synthesised from three different coal waste in South Africa. *Fuel* **2020**, *267*, No. 117157.

(5) Alcañiz-Monge, J.; Lozano-Castelló, D.; Cazorla-Amorós, D.; Linares-Solano, A. Fundamentals of methane adsorption in microporous carbons. *Microporous Mesoporous Mater.* **2009**, *124*, 110−6.

(6) Prauchner, M. J.; Rodriguez-Reinoso, F. Preparation of granular activated carbons for adsorption of natural gas. *Microporous Mesoporous Mater.* **2008**, *109*, 581−4.

(7) Lozano-Castelló, D.; Alcaniz-Monge, J.; De la Casa-Lillo, M.; Cazorla-Amoros, D.; Linares-Solano, A. Advances in the study of methane storage in porous carbonaceous materials. *Fuel* **2002**, *81*, 1777−803.

(8) Arami-Niya, A.; Daud, W. M. A. W.; Mjalli, F. S.; Abnisa, F.; Shafeeyan, M. S. Production of microporous palm shell based activated carbon for methane adsorption: modeling and optimization using response surface methodology. *Chem. Eng. Res. Des.* **2012**, *90*, 776−84.

(9) Sreńscek-Nazzal, J.; Kamińska, W.; Michalkiewicz, B.; Koren, Z. C. Production, characterization and methane storage potential of KOH-activated carbon from sugarcane molasses. *Ind. Crops Prod.* **2013**, *47*, 153−9.

(10) Thu, K.; Kim, Y.-D.; Ismil, A. B.; Saha, B. B.; Ng, K. C. Adsorption characteristics of methane on Maxsorb III by gravimetric method. *Appl. Therm. Eng.* **2014**, *72*, 200−5.

(11) Chakraborty, A.; Saha, B. B.; Ng, K. C.; Koyama, S.; Srinivasan, K. Theoretical insight of physical adsorption for a single-component adsorbent+ adsorbate system: I. Thermodynamic property surfaces. *Langmuir* **2009**, *25*, 2204−11.

(12) Srinivasan, K.; Saha, B. B.; Ng, K. C.; Dutta, P.; Prasad, M. A method for the calculation of the adsorbed phase volume and pseudo-saturation pressure from adsorption isotherm data on activated carbon. *Phys. Chem. Chem. Phys.* **2011**, *13*, 12559−70.

(13) Zhu, Z.; Zheng, Q. Methane adsorption on the graphene sheets, activated carbon, and carbon black. *Appl. Therm. Eng.* **2016**, *108*, 605−13.

(14) Luo, J.; Liu, Y.; Sun, W.; Jiang, C.; Xie, H.; Chu, W. Influence of structural parameters on methane adsorption over activated carbon: evaluation by using D−A model. *Fuel* **2014**, *123*, 241−7.

(15) Ruthven, D. M. *Principles of Adsorption, and Adsorption Processes*; John Wiley & Sons, 1984.

(16) Builes, S.; Sandler, S. I.; Xiong, R. Isosteric heats of gas, and liquid adsorption. *Langmuir* **2013**, *29*, 10416−22.

(17) Saha, B. B.; Koyama, S.; El-Sharkawy, I. I.; Habib, K.; Srinivasan, K.; Dutta, P. Evaluation of adsorption parameters and heats of

adsorption through desorption measurements. *J. Chem. Eng. Data* **2007**, *52*, 2419−24.
(18) Chakraborty, A.; Saha, B. B.; Koyama, S.; Ng, K. On the thermodynamic modeling of the isosteric heat of adsorption and comparison with experiments. *Appl. Phys. Lett.* **2006**, *89*, No. 171901.
(19) Balathanigaimani, M. S.; Kang, H.-C.; Shim, W.-G.; Kim, C.; Lee, J.-W.; Moon, H. Preparation of powdered activated carbon from rice husk and its methane adsorption properties. *Korean J. Chem. Eng.* **2006**, *23*, 663−8.
(20) Ning, P.; Li, F.; Yi, H.; Tang, X.; Peng, J.; Li, Y.; He, D.; Deng, H. Adsorption equilibrium of methane and carbon dioxide on microwave-activated carbon. *Sep. Purif. Technol.* **2012**, *98*, 321−6.
(21) Whittaker, P. B.; Wang, X.; Regenauer-Lieb, K.; Chua, H. T. Predicting isosteric heats for gas adsorption. *Phys. Chem. Chem. Phys.* **2013**, *15*, 473−82.
(22) Herdes, C.; Ferreiro-Rangel, C. A.; Düren, T. Predicting neopentane isosteric enthalpy of adsorption at zero coverage in MCM-41. *Langmuir* **2011**, *27*, 6738−43.
(23) Birkett, G.; Do, D. Correct procedures for the calculation of heats of adsorption for heterogeneous adsorbents from molecular simulation. *Langmuir* **2006**, *22*, 9976−81.
(24) Whittaker, P. B. Predicting the Heats of Adsorption for Gas Physisorption from Isotherm Measurements. Doctoral Dissertation, University of Western Australia: Australia, 2015.
(25) Abdulsalam, J.; Mulopo, J.; Oboirien, B.; Bada, S.; Falcon, R. Experimental evaluation of activated carbon derived from South Africa discard coal for natural gas storage. *Int. J. Coal Sci. Technol.* **2019**, *6*, 459−77.
(26) Omri, A.; Benzina, M. Characterization of activated carbon prepared from a new raw lignocellulosic material: Ziziphus spina-christi seeds. *J. Soc. Chim. Tunis.* **2012**, *14*, 175−83.
(27) Lillo-Ródenas, M. A.; Cazorla-Amorós, D.; Linares-Solano, A. Understanding chemical reactions between carbons and NaOH and KOH: an insight into the chemical activation mechanism. *Carbon* **2003**, *41*, 267−75.
(28) Linares-Solano, A.; Lillo-Ródenas, M.; Marco-Lozar, J. P.; Kunowsky, M.; Romero-Anaya, A. J. NaOH, and KOH for preparing activated carbons used in energy and environmental applications. *Int. J. Energy Environ. Econ.* **2012**, *20*, 355.
(29) Thommes, M.; Kaneko, K.; Neimark, A. V.; Olivier, J. P.; Rodriguez-Reinoso, F.; Rouquerol, J.; Sing, K. S. Physisorption of gases, with special reference to the evaluation of surface area and pore size distribution (IUPAC Technical Report). *Pure Appl. Chem.* **2015**, *87*, 1051−69.
(30) Zhao, W.; Fierro, V.; Zlotea, C.; Aylon, E.; Izquierdo, M.; Latroche, M.; Celzard, A. Optimization of activated carbons for hydrogen storage. *Int. J. Hydrogen Energy* **2011**, *36*, 11746−51.
(31) Hu, Z.; Srinivasan, M. P.; Ni, Y. Preparation of mesoporous high-surface-area activated carbon. *Adv. Mater.* **2000**, *12*, 62−5.
(32) Sing, K.; Everett, D.; Haul, R.; Moscou, L.; Pierotti, R.; Rouquerol, J.; Siemieniewska, T. International union of pure and applied chemistry, IUPAC. *Pure Appl. Chem.* **1985**, *57*, 603.
(33) Panella, B.; Hirscher, M.; Roth, S. Hydrogen adsorption in different carbon nanostructures. *Carbon* **2005**, *43*, 2209−14.
(34) Bénard, P.; Chahine, R. Storage of hydrogen by physisorption on carbon and nanostructured materials. *Scr. Mater.* **2007**, *56*, 803−8.
(35) Düren, T.; Sarkisov, L.; Yaghi, O. M.; Snurr, R. Q. Design of new materials for methane storage. *Langmuir* **2004**, *20*, 2683−9.
(36) Loh, W. S.; Rahman, K. A.; Chakraborty, A.; Saha, B. B.; Choo, Y. S.; Khoo, B. C.; Ng, K. C. Improved isotherm data for adsorption of methane on activated carbons. *J. Chem. Eng. Data* **2010**, *55*, 2840−7.
(37) Martin, A.; Loh, W. S.; Rahman, K. A.; Thu, K.; Surayawan, B.; Alhamid, M. I.; Ng, K. C. Adsorption isotherms of CH4 on activated carbon from Indonesian low grade coal. *J. Chem. Eng. Data* **2011**, *56*, 361−7.
(38) Rahman, K. A.; Chakraborty, A.; Saha, B. B.; Ng, K. C. On thermodynamics of methane+ carbonaceous materials adsorption. *Int. J. Heat Mass Transfer* **2012**, *55*, 565−73.
(39) Do, D. D. *Adsorption Analysis: Equilibria and Kinetics*; Imperial College Press: London, 1998; *Vol. 2*.
(40) Loh, W. S.; Kumja, M.; Rahman, K. A.; Ng, K. C.; Saha, B. B.; Koyama, S.; El-Sharkawy, I. I. Adsorption parameter, and heat of adsorption of activated carbon/HFC-134a pair. *Heat Transfer Eng.* **2010**, *31*, 910−6.
(41) Delavar, M.; Ghoreyshi, A. A.; Jahanshahi, M.; Khalili, S.; Nabian, N. Equilibria and kinetics of natural gas adsorption on multi-walled carbon nanotube material. *RSC Adv.* **2012**, *2*, 4490−7.
(42) Rodrigues, L. A.; da Silva, M. L. C. P. Thermodynamic and kinetic investigations of phosphate adsorption onto hydrous niobium oxide prepared by homogeneous solution method. *Desalination* **2010**, *263*, 29−35.
(43) Whittaker, P. B. Predicting the Heats of Adsorption for Gas Physisorption from Isotherm Measurements. Doctoral Thesis, The University of Western Australia: Australia, 2015.
(44) Aremu, T. *Predicting the Isosteric Heat for Gas Adsorption Studies*; University of Western Australia, 2015.
(45) Choudhary, V. R.; Mayadevi, S. Adsorption of methane, ethane, ethylene, and carbon dioxide on silicalite-l. *Zeolites* **1996**, *17*, 501−7.
(46) Pillai, R. S.; Peter, S. A.; Jasra, R. V. Adsorption of carbon dioxide, methane, nitrogen, oxygen, and argon in NaETS-4. *Microporous Mesoporous Mater.* **2008**, *113*, 268−76.
(47) Grey, T.; Travis, K.; Gale, J.; Nicholson, D. A comparative simulation study of the adsorption of nitrogen and methane in siliceous heulandite and chabazite. *Microporous Mesoporous Mater.* **2001**, *48*, 203−9.
(48) Himeno, S.; Tomita, T.; Suzuki, K.; Yoshida, S. Characterization and selectivity for methane and carbon dioxide adsorption on the all-silica DD3R zeolite. *Microporous Mesoporous Mater.* **2007**, *98*, 62−9.
(49) Lee, J.-W.; Kang, H.-C.; Shim, W.-G.; Kim, C.; Moon, H. Methane adsorption on multi-walled carbon nanotube at (303.15, 313.15, and 323.15) K. *J. Chem. Eng. Data* **2006**, *51*, 963−7.
(50) Zheng, Y.; Li, Q.; Yuan, C.; Tao, Q.; Zhao, Y.; Zhang, G.; Liu, J.; Qi, G. Thermodynamic analysis of high-pressure methane adsorption on coal-based activated carbon. *Fuel* **2018**, *230*, 172−84.
(51) Prasetyo, I.; Do, D. Adsorption rate of methane and carbon dioxide on activated carbon by the semi-batch constant molar flow rate method. *Chem. Eng. Sci.* **1998**, *53*, 3459−67.
(52) Walton, K. S.; Cavalcante, C. L.; Levan, M. D. Adsorption equilibrium of alkanes on a high surface area activated carbon prepared from Brazilian coconut shells. *Adsorption* **2005**, *11*, 107−11.
(53) Tóth, J. State equation of the solid-gas interface layers. *Acta Chim. Hung.* **1971**, *69*, 311−28.
(54) Luo, J.; Liu, Y.; Jiang, C.; Chu, W.; Jie, W.; Xie, H. Experimental and modeling study of methane adsorption on activated carbon derived from anthracite. *J. Chem. Eng. Data* **2011**, *56*, 4919−26.
(55) Rahman, K. A.; Loh, W. S.; Yanagi, H.; Chakraborty, A.; Saha, B. B.; Chun, W. G.; Ng, K. C. Experimental adsorption isotherm of methane onto activated carbon at sub-and supercritical temperatures. *J. Chem. Eng. Data* **2010**, *55*, 4961−7.
(56) Dubinin, M.; Astakhov, V. *Description of Adsorption Equilibria of Vapors on Zeolites over Wide Ranges of Temperature and Pressure*; ACS Publications, 1971.
(57) Saha, B. B.; Uddin, K.; Pal, A.; Thu, K. Emerging sorption pairs for heat pump applications: An overview. *JMST Adv.* **2019**, 1−20.
(58) Tóth, J. Thermodynamical correctness of gas/solid adsorption isotherm equations. *J. Colloid Interface Sci.* **1994**, *163*, 299−302.

https://dx.doi.org/10.1021/acsomega.0c04744
ACS Omega 2020, 5, 32530−32539